PRAMANA — journal of physics

Vol. 76, No. 1
January 2011
pp. 139–147

Role of correlated hopping in mixed valence phenomena

N K GHOSH*, S K BHOWMICK and N S MONDAL
Department of Physics, University of Kalyani, Kalyani 741 235, India
*Corresponding author. E-mail: nanda.ku@rediffmail.com

MS received 27 February 2010; revised 17 May 2010; accepted 17 June 2010

Abstract. Role of correlated hopping is studied using extended Falicov–Kimball model in a small cluster. A discontinuous insulator-to-metal transition is observed at a critical f-level energy. Transition is sharper for larger correlated hopping. In the specific heat curves a two-peak structure consisting of a sharp peak followed by a Schottky-type broad peak is exhibited. In a limited parameter region, some heavy-fermion like characteristics have been observed.

Keywords. Mixed valent systems; Falicov–Kimball model; correlated hopping.

PACS Nos 71.30.+h; 71.10.-w; 71.10.Hf

1. Introduction

Many have studied the phenomena of valence transition [1–3]. The Falicov–Kimball model (FKM) [4] has become an important theoretical model for describing valence transition and other anomalous properties of correlated fermions on a lattice. The model is characterized by the co-existence of two different electronic states; one is the localized highly correlated ion-like states and the other is extended, uncorrelated, Bloch-like states. It is well accepted that many of the anomalous features, e.g., mixed valence (MV) phenomena, metal insulator (MI) transitions, originate from a change in the occupation numbers of electronic states. This model successfully explains intermediate valence transitions as observed in certain rare-earth compounds. For strong interactions, it demonstrates a discontinuous insulator–insulator transition [5], and for weak interactions it shows a discontinuous insulator–metal transition [6]. Finite-temperature calculations on the model also provide an explanation for the anomalously large values of the specific heat coefficients [7] and extremely large changes of electrical conductivity [8] found in some intermediate-valence compounds (SmB_6).

Besides the above-mentioned works, there are many and different applications of quantum many-body models. In [9], authors performed density matrix renormalization group (DMRG) calculations to study electric field-induced insulator–metal transition in one-dimensional Mott–Peierls chains. It is well established that the quantum many-body configuration interaction method captures the low-energy properties of the nanoscale

systems such as graphene [10]. The properties of the ground state and the low-lying excited states of the spin-1 and spin-$\frac{1}{2}$ alternating chains with nearest-neighbour antiferromagnetic and next-nearest-neighbour ferromagnetic interactions have also been studied [11] by applying the spin-wave theory and DMRG methods. Further, in an attempt to understand the mechanism of charge transport through DNA, Mallajosyula *et al* [12] combined molecular dynamics simulations and density functional theory to analyse the electrical structure and transmission probability in four different DNA sequences under physiological conditions. They successfully explained recent length-dependent conductance data for individual DNA molecules in water.

Present paper deals with the study of MV phenomena. But, a large number of works on the issue are sensitive to the approximations used [13,14]. Numerous approximate results and some exact calculations [7] reported upto now have established a good basis for further realistic extension of the model. Inclusion of correlated hopping term [15] substantially changed the ground-state properties of this model in two dimensions. The ground state phase diagram and the characteristic metal–insulator transitions are largely modified when correlated hopping term is added to conventional FKM.

In this work, we have studied the role of correlated hopping, on-site Coulomb interaction and hybridization on valence transition. The effect of correlated hopping on specific heat is also studied. For this, we have considered a four-site two-dimensional square cluster. A two-band FKM extended by hybridization and correlated hopping is taken. Observations have been compared with the existing results.

2. Formulation

Our starting Hamiltonian has the form

$$H = H_0 + H_{\rm corr}, \tag{1}$$

where

$$\begin{aligned} H_0 \;=\; & E\sum_{i\sigma} f^\dagger_{i\sigma} f_{i\sigma} + U\sum_{i} f^\dagger_{i\uparrow} f_{i\uparrow} f^\dagger_{i\downarrow} f_{i\downarrow} + G\sum_{i\sigma\sigma'} d^\dagger_{i\sigma} d_{i\sigma} f^\dagger_{i\sigma'} f_{i\sigma'} \\ & + V\sum_{\langle i,j\rangle\sigma} (f^\dagger_{i\sigma} d_{j\sigma} + d^\dagger_{j\sigma} f_{i\sigma}) + t\sum_{\langle i,j\rangle\sigma} d^\dagger_{i\sigma} d_{j\sigma}. \end{aligned} \tag{2}$$

The summations extend over all pairs of nearest-neighbour sites on a simple two-dimensional square lattice; $f_{i\sigma}$ and $d_{i\sigma}$ are the usual fermion operators for *f*- and *d*-electrons respectively ($\sigma, \sigma' = \text{spin}$), *E* is the *f*-level energy, *G* is the strength of the *f–d* Coulomb interaction, *U* is the on-site Coulomb interaction and *V* is the *f–d* hybridization interaction. The last term is the kinetic energy corresponding to quantum-mechanical hopping of the itinerant *d*-electrons between nearest-neighbour sites.

$$H_{\rm corr} = t'\sum_{\langle i,j\rangle\sigma} (f^\dagger_{i\sigma} f_{i\sigma} + f^\dagger_{j\sigma} f_{j\sigma}) d^\dagger_{i\sigma} d_{j\sigma}, \tag{3}$$

where $H_{\rm corr}$ is the correlated hopping term with interaction strength t'. The representative four-site spin state is taken in the form

$$|\, n^f_{1\uparrow} n^f_{1\downarrow} n^d_{1\uparrow} n^d_{1\downarrow} n^f_{2\uparrow} n^f_{2\downarrow} n^d_{2\uparrow} n^d_{2\downarrow} n^f_{3\uparrow} n^f_{3\downarrow} n^d_{3\uparrow} n^d_{3\downarrow} n^f_{4\uparrow} n^f_{4\downarrow} n^d_{4\uparrow} n^d_{4\downarrow}\rangle. \tag{4}$$

There are totally 120 basis states and the eigenvectors of *H* are represented as a linear combination of vectors (4). *f*-electron density $\langle n_i^f \rangle = (1/N) \sum_{i\sigma} f_{i\sigma}^\dagger f_{i\sigma}$ where *N* is the number of lattice sites; *f–d* intersite correlation function $c_{fd} = \langle f_{i\sigma}^\dagger d_{j\sigma} \rangle$. Low-temperature specific heat is calculated using the relation

$$C = k_{\mathrm{B}} \beta^2 \frac{\partial^2}{\partial \beta^2} \ln Z, \tag{5}$$

where $Z = \sum_\alpha \mathrm{e}^{-\beta E_\alpha}$, the sum is taken over all eigenstates, E_αs are the eigenvalues and $\beta = 1/k_{\mathrm{B}}T$, k_{B} being the Boltzmann constant.

3. Results and discussions

Figure 1 shows the variation of $\langle n_i^f \rangle$ with *E* for different values of t'. It appears from the figure that the transition is sharper for larger t' at the critical $E = E_{\mathrm{c}} = -2$. The following selection of hopping matrix amplitudes $t = -1$ and $t' > 0$ could lead to the instability of the CDW state and thereby to an insulator-to-metal transition. It is also remarkable that even in this strong coupling limit ($U = 5$), the correlated hopping can favour insulator–metal transition where the ground states of the conventional FKM are insulating for all *f*-electron densities. Our result is totally in agreement with [16].

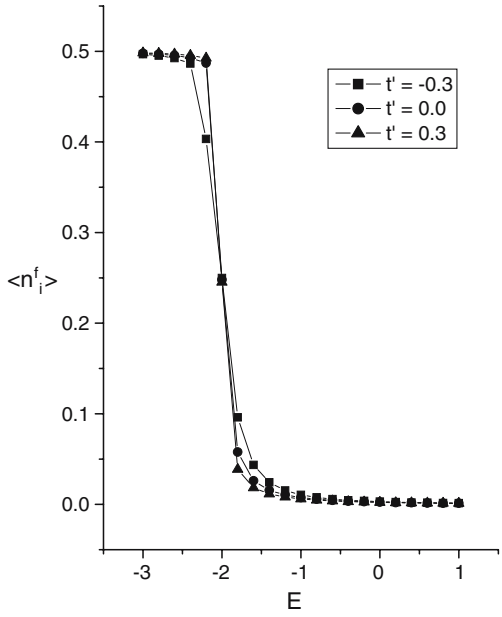

Figure 1. $\langle n_i^f \rangle$ vs. E for different correlated hopping strength t'. Here $V = 0.1$, $U = 5$, $G = 2$, $t = -1$.

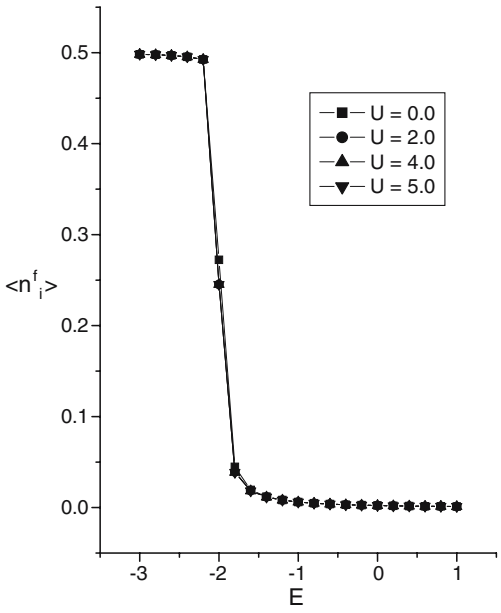

Figure 2. $\langle n_i^f \rangle$ vs. E for different values of U. Here $V = 0.1$, $G = 2$, $t = -1$, $t' = 0.3$.

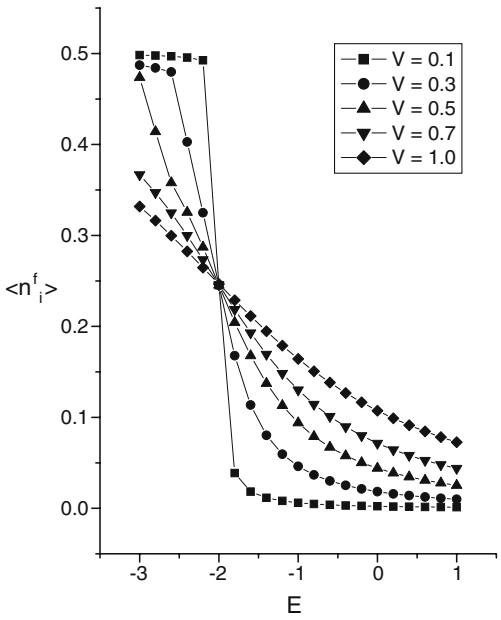

Figure 3. $\langle n_i^f \rangle$ vs. E for different values of V. Here $U = 5$, $G = 2$, $t = -1$, $t' = 0.3$.

But, if $\langle n_i^f \rangle$ is plotted with *E* for different values of *U* (figure 2), we observe that the characteristics of the valence transition do not change significantly. $E_c = -2$ remains the same, but the transition looks slightly sharper for higher values of *U*.

To understand the role of hybridization on valence transition, we have plotted $\langle n_i^f \rangle$ vs. *E* for varying *V* from 0.1 to 1.0 in figure 3. It is apparent from the figure that discontinuous valence transition appears for smaller hybridization at $E = E_c = -2$. This is in accordance with the results based on the alloy-analog approximation [17] and small-cluster exact-diagonalization calculations [18].

In figure 4, we have plotted c_{fd} vs. *E* for different correlated hopping strengths. The intermediate-valence state is normally characterized by a non-zero value of this correlation function [19]. With the increase of *E*, the correlation function decreases from a value close to zero, and after a certain *E* value, increases towards zero. This is probably due to the fact that in the insulating or metallic phase this correlation function should approach zero. The correlation function increases with the increase of t'. For large negative *E*, correlated hopping keeps the system closer to the insulating phase, and after the transition keeps the system closer to the metallic phase. In both the cases $\langle f_{i\sigma}^{\dagger} d_{j\sigma} \rangle$ should be closer to zero than that for smaller t' as is apparent from the figure.

That the characteristics of the valence transition does not change significantly is also apparent from figure 5 where c_{fd} is plotted against *E* for different values of *U*. The value of the correlation c_{fd} is slightly closer to zero in the insulating or metallic phase for higher values of *U*, confirming the observation from figure 2.

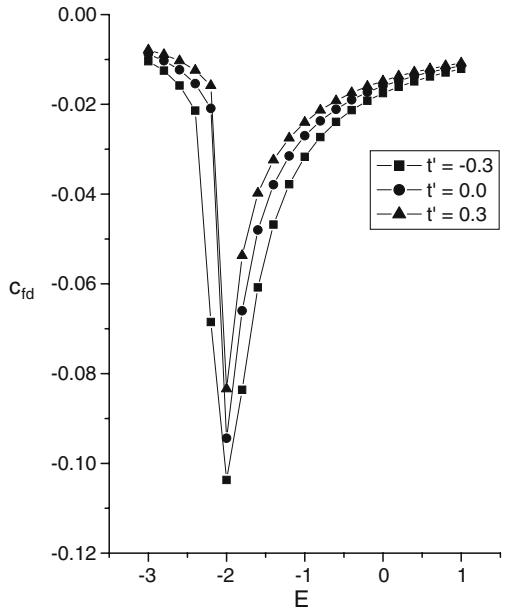

Figure 4. C_{fd} vs. *E* for different values of t'. Here $V = 0.1, U = 5, G = 2, t = -1$.

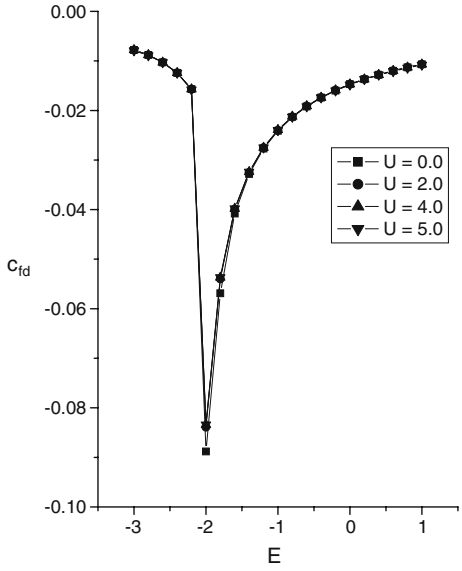

Figure 5. C_{fd} vs. E for different values of U. Here $V = 0.1$, $G = 2$, $t = -1$, $t' = 0.3$.

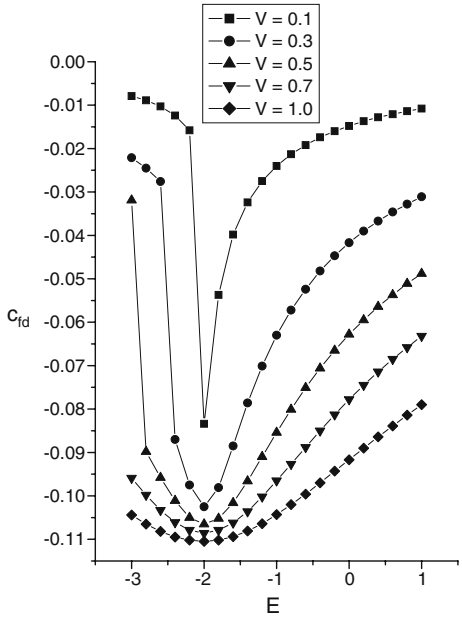

Figure 6. C_{fd} vs. E for different values of V. Here $U = 5$, $G = 2$, $t = -1.0$, $t' = 0.3$.

The observation of figure 3 is also supported in figure 6, which shows that for large negative *E*, lower *f–d* hybridization maintains the system closer to the insulating phase and after the transition at $E = E_{\rm c}$, keeps it closer to the metallic phase. So, increased hybridization smears the discontinuous transition [18].

Variation of low-temperature specific heat ($k_{\rm B}$ is taken as unity) with temperature is shown in figures 7 and 8. The specific heat curves fall into two principal categories according to whether there are one or two peaks. When $E > E_{\rm c}$, a broad single peak structure is obtained [20]. The peak shifts to higher temperature region with the increase of correlation strength. Figure 8 shows that the specific heat curves exhibit a two-peak structure [21] with $E \leq E_{\rm c}$. The first sharp peak is due to a large number of many-body states, which are nearly degenerate with the ground state. The second peak (Schottky-type) at higher temperature is due to the distribution of the many-body states like binomial distribution. Curves also confirm the non-Fermi liquid behaviour of the system.

We have plotted γ against *T* in figure 9. At the low-temperature region considered here, the specific heat curve follow: $\mathrm{C} = \gamma T + \beta T^3$. The values of specific heat coefficient γ as obtained from figure 7 are plotted against *T* in figure 9. γ increases at lower temperatures, attains a peak value, and then gradually decreases with *T*. Peak value of γ is enhanced with t', thereby indicating the presence of more many-body states. This rise in the value of γ declares the onset of heavy-fermion behaviour [22].

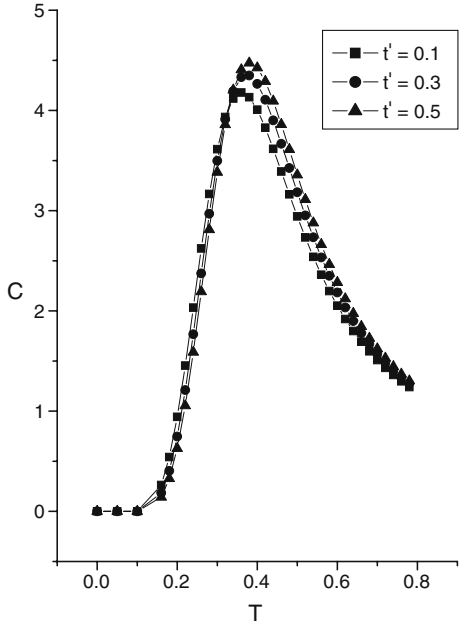

Figure 7. Specific heat vs. temperature for different t'. Here $E = -1$, $V = 0.1$, $U = 5$, $G = 2$, $t = -1$.

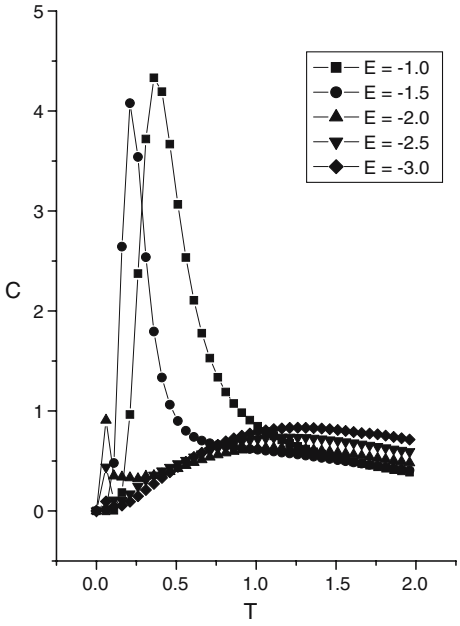

Figure 8. Specific heat vs. temperature for different E. Here $V = 0.1$, $U = 5$, $G = 2$, $t' = 0.3$, $t = -1$.

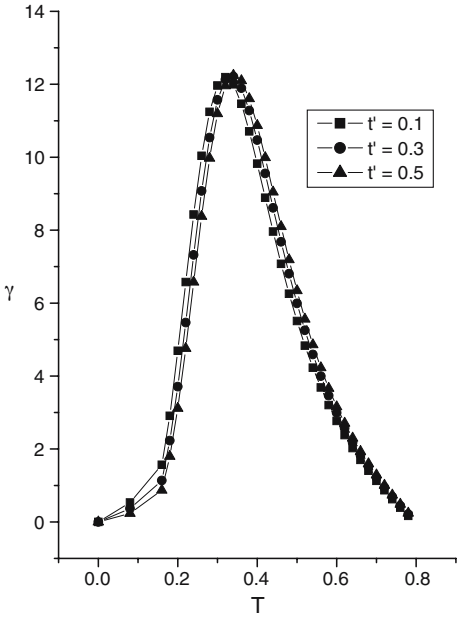

Figure 9. Specific heat coefficient vs. T for different t'. Here $E = -1$, $V = 0.1$, $U = 5$, $G = 2$, $t = -1$.

4. Conclusion

In summary, the role of correlated hopping, on-site Coulomb interaction, and *f–d* hybridization in mixed valence phenomena has been studied using extended Falicov–Kimball model. Dependence of *f*-state occupation and *f–d* intersite correlation on *f*-level energy has been observed. It appears that a discontinuous insulating-to-metal transition occurs at a critical *f*-level energy. Temperature dependence of specific heat shows both single peak as well as double peak structures. Peak value of the specific heat coefficient γ is enhanced with correlated hopping. When *f*-level energy is near critical $E = E_{\rm c}$, a two-peak structure consisting of a sharp peak followed by a broad peak (of Schottky-type) is observed. Some features of the heavy-fermion systems are also observed in a limited parameter region.

Acknowledgement

The authors are thankful to the University of Kalyani for financial help.

References

[1] C M Varma, *Rev. Mod. Phys.* **48**, 219 (1976)
[2] N K Ghosh, S C Ghosh and R L Sarkar, *Phys. Status Solidi* **B171**, 107 (1992)
[3] H Cencarikova, P Farkasovsky and M Zonda, *Acta Phys. Polon.* **A113**, 287 (2008)
[4] L M Falicov and J C Kimball, *Phys. Rev. Lett.* **22**, 997 (1969)
[5] P Farkasovsky, *Phys. Rev.* **B51**, 1507 (1995)
[6] P Farkasovsky, *Phys. Rev.* **B52**, R5463 (1995)
[7] N K Ghosh and R L Sarkar, *Phys. Status Solidi* **B176**, 395 (1993)
[8] P Farkasovsky, *Z. Phys.* **B102**, 91 (1997)
[9] S Dutta, S Lakshmi and S K Pati, *J. Phys.: Condens. Matter* **19**, 322201 (2007)
[10] S Dutta, S Lakshmi and S K Pati, *Phys. Rev.* **B77**, 073412 (2008)
[11] S Mohakud and S K Pati, *Phys. Rev.* **B76**, 014435 (2007)
[12] S S Mallajosyula, J C Lin, D L Cox, S K Pati, and R R P Singh, *Phys. Rev. Lett.* **101**, 176805 (2008)
[13] I Singh, A K Ahuja and S K Joshi, *Solid State Commun.* **34**, 65 (1980)
[14] J Zielinski and P Trzaskoma, *Solid State Commun.* **39**, 849 (1981)
[15] H Cencarikova and P Farkasovsky, *Physica* **B359**, 690 (2005)
[16] P Farkasovsky and N Hudakova, *J. Phys.: Condens. Matter* **14**, 499 (2002)
[17] G Czycholl, *Phys. Rep.* **246**, 401 (1986)
[18] P Farkasovsky, *Z. Phys.* **B104**, 553 (1997)
[19] P Entel, H J Leder and N Grewe, *Z. Phys.* **B30**, 277 (1978)
[20] J M Lawrence, P S Riseborough and R D Parks, *Rep. Prog. Phys.* **44**, 1 (1981)
[21] S D Bader, N E Phillips and D B McWhan, *Phys. Rev.* **B7**, 4686 (1973)
[22] C Kittel, *Introduction to solid state physics*, 7th edn (Wiley India Pvt. Ltd., New Delhi, 2007) p. 156